

## Supplementary Material

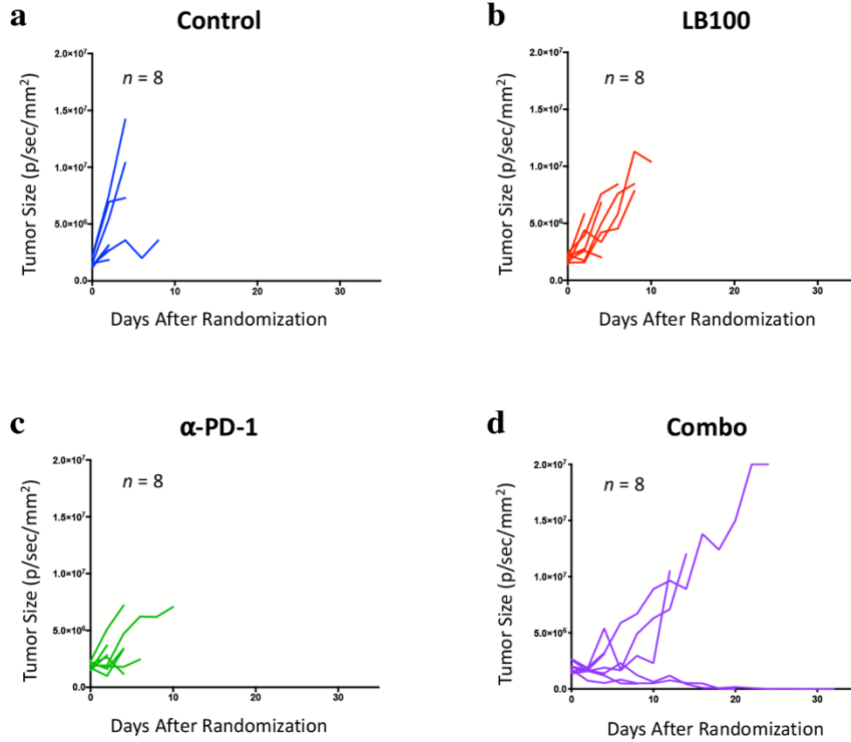
Antibody (flow)	Clone	Fluorophore	Dilution	Isotype
CD3e	145-2C11	PE	1:40	Armenian Hamster IgG
CD4	RM4-5	AF647	1:333	Rat IgG2 $\alpha$ κ
CD8a	53-6.7	BUV737	1:40	Rat IgG2 $\alpha$ κ
CD8b.2	53-5.8	FITC	1:100	Rat IgG1κ
CD11b	M1/70	BUV395	1:80	Rat IgG2 $\beta$ κ
CD11c	HL3	AF700	1:40	Armenian Hamster IgG1, $\lambda$ 2
CD11c	HL3	BUV737	1:40	Armenian Hamster IgG1, $\lambda$ 2
CD19	1D3	BB515	1:40	Rat IgG2 $\alpha$ κ
CD25	PC61	BV605	1:160	Rat IgG1 $\lambda$
CD44	IM7	BV421	1:80	Rat IgG2 $\beta$ κ
CD45	30-F11	BV785	1:160	Rat IgG2 $\beta$ κ
CD62L	MEL-14	BUV395	1:80	Rat IgG2 $\alpha$ κ
CD161 (NK1.1)	PK136	BUV395	1:40	Mouse IgG2 $\alpha$ κ
CD161 (NK1.1)	PK136	BV421	1:80	Mouse IgG2 $\alpha$ κ
CD206 (mannose receptor)	MR5D3	AF647	1:80	Rat IgG2 $\alpha$
F4/80	BM8	PerCP/Cy5.5	1:200	Rat IgG2 $\alpha$ κ
Foxp3	MF23	BV421	1:80	Rat IgG2 $\beta$
IFN- $\gamma$	XMG1.2	BV605	1:20	Rat IgG1κ
IFN- $\gamma$	XMG1.2	PE	1:80	Rat IgG1κ
Ki-67	B56	PerCP/Cy5.5	1:40	Mouse IgG1κ
Ly-6C	AL-21	PerCP/Cy5.5	1:20	Rat IgMκ
Ly-6G	1A8	AF488	1:100	Rat IgG2 $\alpha$ κ
LY-6G	1A8	BV605	1:80	Rat IgG2 $\alpha$ κ
T-bet	4B10	AF700	1:80	Mouse IgG1κ
TNF- $\alpha$	MP6-XT22	BV510	1:40	Rat IgG1

Blocking Antibody	Clone	Dilution
True-Stain Monocyte Blocker	n/a	1:20
CD16/32	93	Rat IgG2 $\alpha$ λ

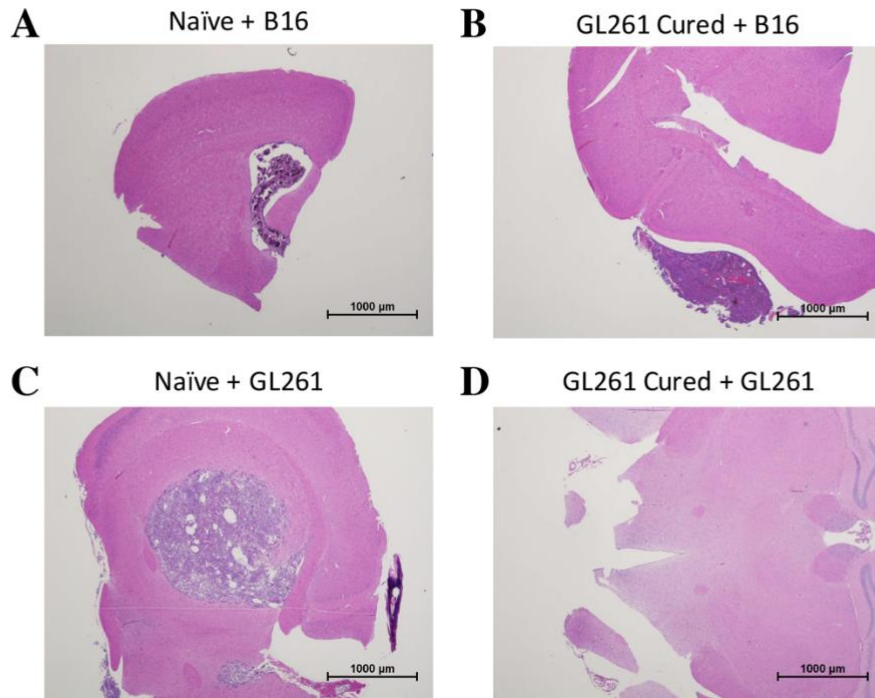
Therapeutic Antibody	Clone	Dose
PD-1	RMP1-14	10 mg/kg
CD8	53.6.7	10 mg/kg
CD4	GK1.5	10 mg/kg

*Antibodies bought from BD Bioscience, Biolegend, Invitrogen, eBioscience, Bio X Cell and Novus*

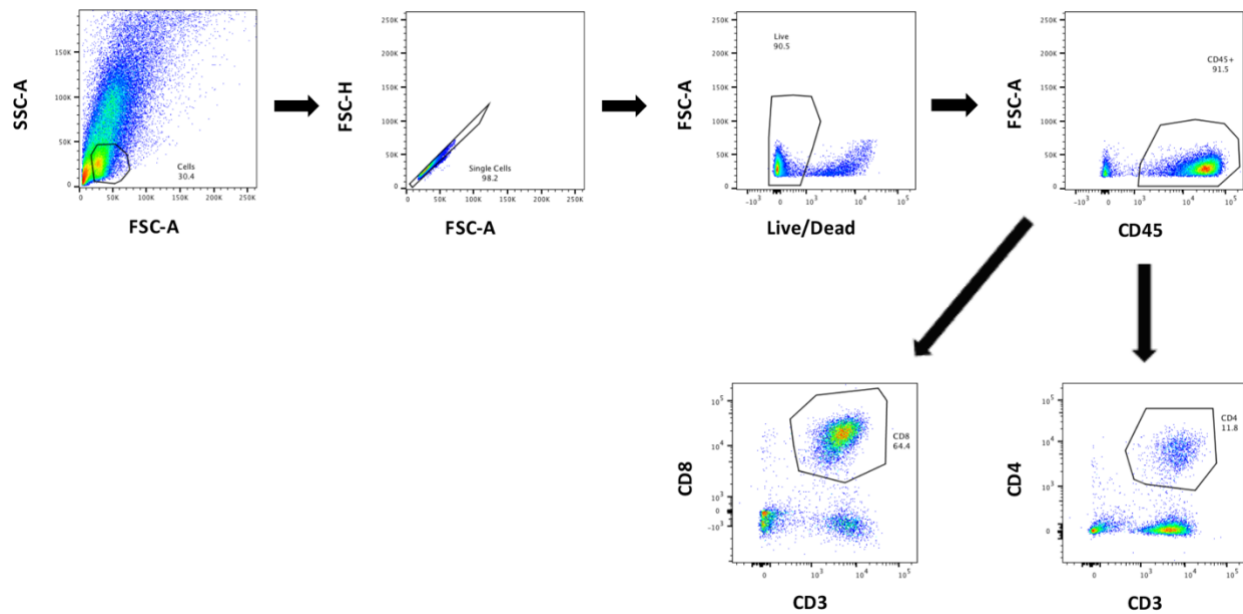
**Supplementary Table 1. Antibodies.** Antibodies used for flow cytometry (clones and dilutions) and therapeutics (clones and dosage)



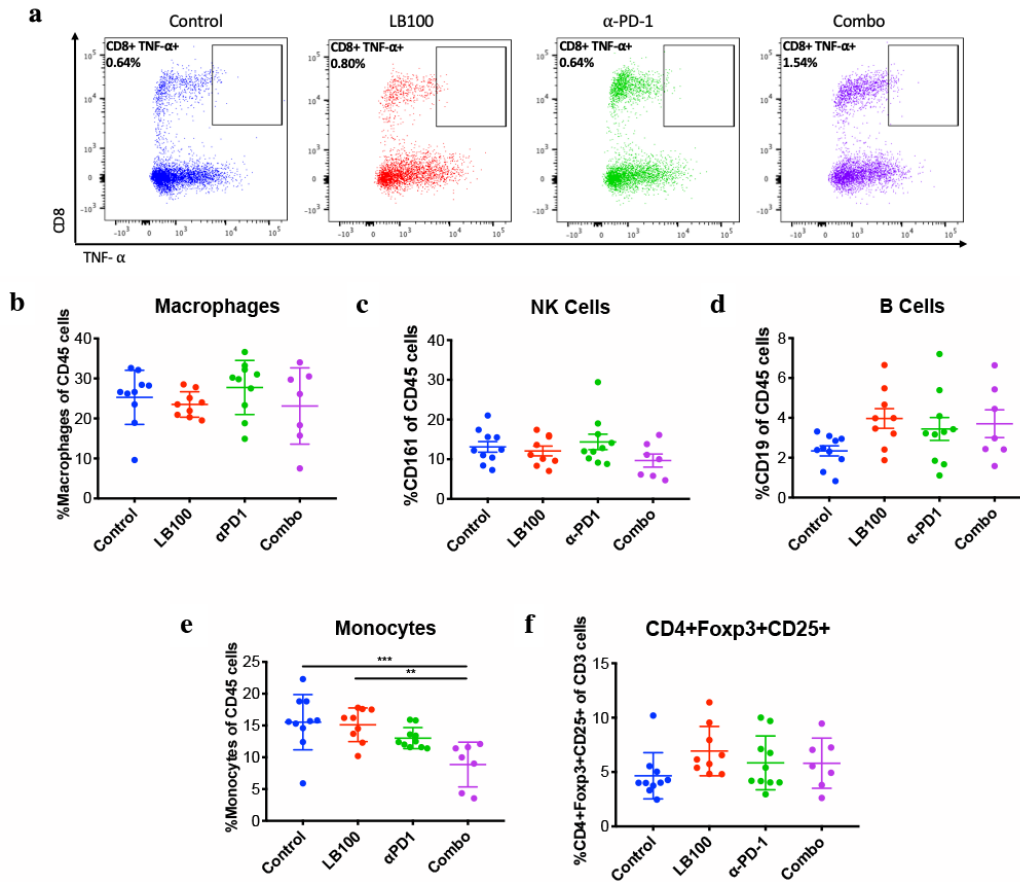
**Supplementary Figure 1. PP2A inhibition and PD1 blockade synergistically elicit tumor rejection in GL261.** Individual tumor growth measured in BLI of the ROI in (a) control (b) LB-100 (c) α-PD-1 and (d) combination groups plotted as days after randomization.



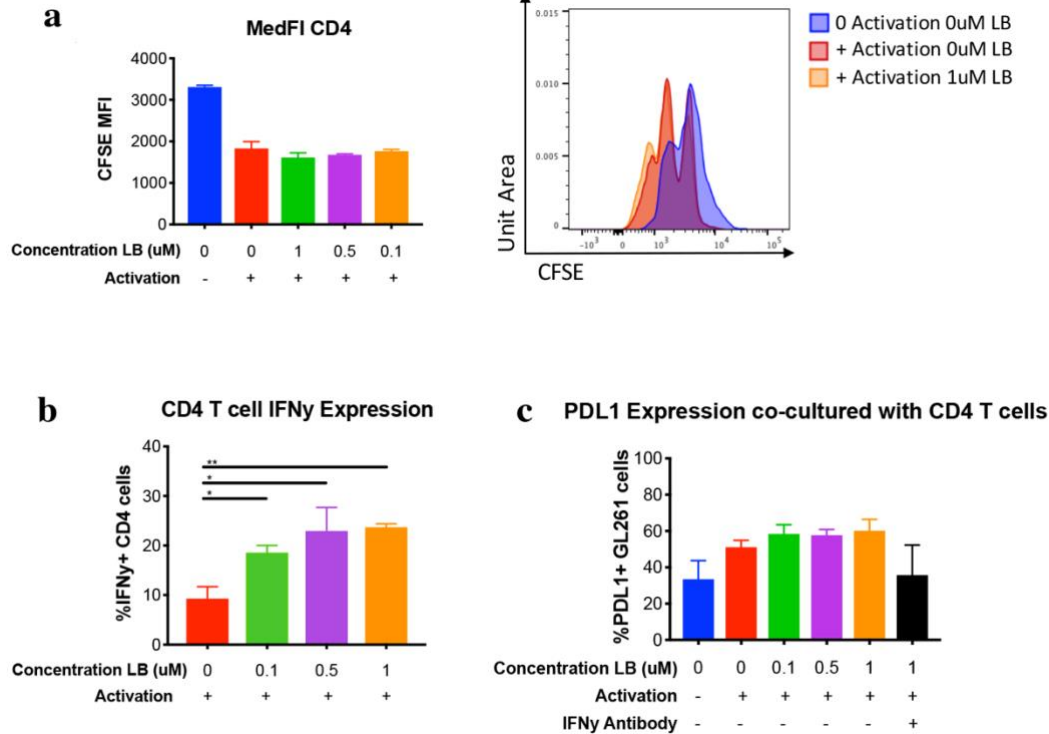
**Supplementary Figure 2. Combination treatment result in a long-term antitumor antigen-specific memory of cured animals.** Representative images of hematoxylin-and-eosin staining of brain specimens from (a) naïve mouse exposed to B16, (b) CR mouse exposed to B16, (c) naïve mouse exposed to GL261 and (d) cured mouse re-exposed to GL261. CR mice re-challenged with GL261 demonstrated no histologic evidence of tumor establishment.



**Supplementary Figure 3. Gating strategy for flow cytometric analysis of tumor infiltrating lymphocytes.** We first used SSC-FSC gate to exclude non-cellular debris, followed by exclusion of duplets by FSC-H-FSA-A gate. Fixable live-dead (L/D) stain was used to exclude dead cells. Live cells were then gated based on expression of CD45+ pan leukocyte marker. CD45- cells were considered as tumor cells. CD45+ cells were then phenotyped further based on CD3, CD8, CD4 expression. CD45+CD3+CD8+ cells were gated as CD8+ lymphocytes, while CD45+CD3+CD4+ cells were gated as CD4+ lymphocytes. Further, staining of the CD4+ and CD8+ subsets were then performed as indicated in the text.



**Supplementary Figure 4. Immune profiling of tumor infiltrating leukocytes.** Combination therapy enhanced CD8+ T cell function but did not alter tumor infiltration of macrophages, natural killer cells or B cells. Monocytes cells were decreased with combination treatment. (a) Representative FACS plots of TNF- $\alpha$ + CD8+ as a percentage of CD45+ cells. (b) Macrophages (CD45+ CD3- CD11c<sup>low</sup> CD11b+ Ly6G- Ly6C<sup>low</sup>) expressed as a percentage of CD45+ cells were not significantly changed in any treatment group. (c) NK (CD45+ CD161+) cells expressed as a percentage of CD45+ cells were not significantly changed in any treatment group. (d) B cells (CD45+ CD19+) expressed as a percentage of CD45+ cells were not significantly changed in any treatment group. (e) Monocytes (CD45+ CD3- CD11c<sup>low</sup> CD11b+ Ly6G- Ly6C<sup>high</sup>) as a percentage of CD45+ cells were significantly decreased in combination compared to control or LB-100 alone. (f) Tregs (FoxP3+ CD25+ CD4+) expressed as a percentage of CD3+ cells were not significantly changed in any treatment group. \*P<0.05 \*\*P<0.01, \*\*\*P<0.001, \*\*\*\*P<0.0001 (one-way ANOVA with Tukey's multiple comparison test). Error bars depict SEM.



**Supplementary Figure 5. LB-100 enhances IFN-gamma secretion of CD4+ T-cells in vitro.** LB-100 did not alter CD4+ T cell proliferation, but increased CD4+ T cell production of IFN-gamma. There was a trend toward increase in tumor PD-L1 expression. (a) LB-100 did not increase proliferation of CD4+ T cells. Flow cytometry analyzing CFSE cytosolic dye as a marker of CD4+ T cell proliferation 72 hours after activation. Representative FACS histogram. (b) LB-100 increased secretion of IFN-gamma by CD4+ T cells. Flow cytometry analyzing expression of IFN-gamma in CD4+ T cells 72 hours after activation in the presence of LB-100 dose titration. (c) Flow cytometry analyzing PD-L1 expression in tumor cells co-cultured with CD4+ T cells exposed to a titration concentration of LB-100. There was a trend, but insignificant, increase in tumor PD-L1 expression with LB-100 treatment. \* $P < 0.05$  \*\* $P < 0.01$  (one-way ANOVA with Tukey's multiple comparison test). Error bars depict SEM.